IOSR Journal Of Pharmacy And Biological Sciences (IOSR-JPBS)
e-ISSN:2278-3008, p-ISSN:2319-7676. Volume 16, Issue 2 Ser. III (Mar. – Apr. 2021), PP 20-30
www.Iosrjournals.Org

Characterization of Porous Borosilicate Bioactive Glasses for Medical Applications

H. Kamal[1,2 *] and Dania Waggas[3]
[1,3] *Fakeeh College for medical sciences-P.O.Box 2537, Jeddah 21461 KSA*
[2]*Physics Department, Faculty of Science, Mansoura University, Mansoura 35516, Egypt*

**Corresponding author: H.Kamal*

Abstract
The preparation of glass scaffolds is mainly effective if we make the glass amorphous after being sintered to preserve both gradual dissolution and conversion to hydroxyapatite. Borosilicate glasses were sintered into a porous scaffold using 70 vol. % ammonium bicarbonate $NH_4(HCO_3)$ as a foaming agent. Glasses were wrinkled and sintered for 2 hours at 10 °C/min heating rate. The Sintering temperatures between 500°C-600°C. The density of the samples decreased as the temperature rose to 580°C. The powders were further mixed with 70 vol. % ammonium bicarbonate $NH_4(HCO_3)$ foaming agent to make highly porous scaffolds needed todifferent medical applications.When comparing samples sintered with ammonium bicarbonate to samples sintered without ammonium bicarbonate the density of the samples sintered with ammonium bicarbonate was found to be lower than samples without ammonium bicarbonate. This means that the samples' porosity has increased.
The borosilicate scaffolds were immersed in SBF to study it's in vitro properties. The pH of the SBF solution containing scaffolds increased due to natural dissolution of this form of glass, resulting in a heavy Na^+/H^+ exchange and a significant alkaline and alkaline ion release. Due to the resulting degradation of these compounds, the borophosphate scaffolds induced a decrease in pH and hence a major release of phosphorus in SBF. SEM/EDS and XRD analysis revealed a reasonable precipitation of hydroxyapatite on borosilicate glass scaffolds, as previously stated. It was discovered that the borophosphate scaffold is more stable and reacts at a slower rate.

Key Words*:Borosilicate, Porosity, Scaffolds, Medical Application*

Date of Submission: 03-04-2021 Date of Acceptance: 17-04-2021

I. Introduction

Porous glasses can be thought of as phase-separated alkali borosilicate glasses' leaching materials[2, 3, 4]. Porous glasses include open-pore glasses made by glass sintering processes and porous silica glass made by the sol–gel method. This researchonly looks at porous glasses made from phase-separated alkali borosilicate glasses.

Phase separation occurs when alkali borosilicate glasses of a suitable composition are heated to temperatures between 500 and 580°C. It is possible toenter two distinct but intertwined stages. The first is a borate that is alkali-rich and soluble in mineral acids, alcohols, and water[3, 5].The second is nearly completely made up of silica. During the leaching process, porous glasses made around complete percentage of silica (96%) are obtained. The original glass composition, thermal treatment conditions (temperature, time), and abrasion are all factors that affect the structural and properties of porous glasses [6, 7].

Microporous glasses are made by heating the original glasses to temperatures between 580 and 700 degrees Celsius. The alkali-rich borate phase formed during this step dissolves silica. Finely scattered silica-gel persists in the pores of the primary silica matrix due to the poor solubility of silica in acidic media, undermining the pore structure of the resulting porous glass. A liquid alkaline solution is used to dissolve colloidal deposits [4]. This method is used in the production of industrial controllable -pore glasses.Biomedical applications have recently prompted the development of bioactive glasses based on borate [1, 2, 5, 8, 9].Based upon immersion of glasses in an aqueous phosphate solution, such as a simulated body fluid, borate glasses can transform faster and more thoroughly to hydroxyapatite (HA) due to their low chemical resistance (SBF) [3, 10, 11, 12].

Many scholars have addressed the kinetics and mechanism of converting glass particles to HA by partially or entirely replacing the SiO_2 content in 45S5 glass with B_2O_3[7, 13, 14, 15, 16, 17].The conversion rate of the glass increased dramatically as the B_2O_3 quality improved in these experiments with glass particles [18, 19].The conversion of porous 3D scaffolds of B2O3-containing glasses with diverse compositions to HA in

an aqueous phosphate solution was recently studied in vitro[20].The effect of the B_2O_3 content of the glass on the deterioration of the scaffolds, on the other hand, has not been thoroughly studied. Furthermore, no research has been done on the impact of B_2O_3 material on essential scaffold conditions for bone regeneration, such as the ability to facilitate osteogenic cell proliferation and function in vitro and tissue penetration in vivo[14, 16, 19].

The aim of this paper is to prepare and characterize borosilicate bioactive glass system, this system was sintered into a porous glass with a 70% ammonium bicarbonate $NH_4(HCO_3)$ foaming agent to make the scaffolds needed in different medical applications.

II. Materials And Methods

The materials that were required for preparation of glasses and scaffolds are listed in table 1 and table 2 below.

Table 1: Glass materials

Glass name	*Chemical composition*
S40B10	$40SiO_2$-$10B_2O_3$-$24Na_2O$-$20CaO$-$6P_2O_5$

Table 2: Composition of S40B10 presented in (Mol. %)

Composition (mol. %)	S40B10
SiO_2	40
Na_2O	24
CaO	20
B_2O_3	10
P_2O_5	6

GLASS AND POWDER PREPARATION

Borosilicate glass starting materials S40B10 were analytical reagent grades Na_2CO_3, H_3BO_3, $CaCO_3$, $CaHPO_4.2H_2O$ and 99.4 percent pure SiO_2. Glass S40B10 had a composition of $40SiO_2$-$10B_2O_3$-$24Na_2O$-$20CaO$-$6P_2O_5$.

A mixture of the appropriate oxides from the starting material in the Alumina crucibles was made and was melted for one hour at 1400°C and 1050°C for glass S40B10. The crushed powders were packed in a tungsten carbide grinding bowl (76 mm) and milled in a planetary ball mill. A 3 wt additive was added for PEG (polyethylene glycol) and Dolapix C64.

After milling, the powder was dried in the oven at 70°C for 24 hrs. The material formed during the drying process was granulated using a porcelain mortar and pestle. The powders were then moved through a stainless-steel sieve of 100 μm using a sieve shaker.The $NH_4(HCO_3)$ foaming agent and the glass powder mixtures were prepared by mixing 2 grams which were rotated at a speed of 96 rpm for 30 minutes where 12 aluminum milling balls (2 mm) The foaming agent ammonium bicarbonate $NH_4(HCO_3)$ was applied with a material of 70 vol.%.To establish porous bioactive glass scaffolds, samples were sintered with and without the foaming agent ammonium bicarbonate $NH_4(HCO_3)$ respectively. Samples with ammonium bicarbonate $NH_4(HCO_3)$ were sintered for 1 hour at 540^{o}C for S40B10 and 500^{o}C after burning with $NH_4(HCO_3)$ foaming agent at 65 ^{o}C for 2 hours.

Scaffolds were treated and immersed in simulated body fluid (SBF) solution at 37°C as suggested by Kokubo et al[21].

Table 4: Ionic concentration of SBF compared to the human blood plasma

	Concentration mM	
	SBF K9	BLOOD PLASMA
Na+	142.0	142.0
K^+	5.0	5.0
Mg^{2+}	1.5	1.5
Ca^{2+}	2.5	2.5
Cl^-	147.8	103.0
$(HCO_3)^-$	4.2	27.0
$(HPO_4)^{2-}$	1.0	1.0
SO_4^{2-}	0.5	0.5

The sample mass to volume of the SBF ratio (1 m1/40mg) was held constant in both experiments. For 24 hours, 48 hours, 72 hours, and 168 hours, 1000 mg of scaffolds is dispersed in the solution. Scaffolds were removed from the solution and dried at 37°C after being rinsed with ethanol to avoid further reactions.

CHARACTERIZATION TECHNIQUES

Thermal Properties

Thermal properties of the glasses (DTA) were calculated using differential thermal analysis. In N_2 atmosphere platinum dishes, measurements were taken on 25 mg samples.The glass transition temperature Tg can be obtained by taking the first derivative of the differential thermal analysis (DTA) curve.

Particle Size Measurements

Particle size measurement was done to determine the size of the particles of the powders needed for sintering.the distribution of particle size was calculated by A Mastersizer-2000 instrument.

Density Measurements

The density of samples was calculated using the Archimedes principle.

XRD Analysis of Powder and Sintered Samples

The crystalline phases that may be formed during the powder preparation process, as well as after sintering and immersion in simulated body fluid, were investigated using the Bruker D2 Phaser XRD analysis method (SBF).The D2 Phaser uses Co k radiation released at 30kV and 10mA.The following criteria were used to take measurements: 2θ value with phase sizes of 0.02° (2θ) varying from 2θ (10° - 90°)

Surface Structural Analysis Using Scanning Electron Microscopy

SEM experiments were carried out on glass samples at room temperature using a Philips XL30 SEM connected to an EDX unit, with a 30kV accelerating voltage and magnification up to 400,000.For morphological investigations, all surfaces of the analyzed samples were coated with gold.

ICP Analysis

Inductively Coupled Plasma analysis on10X diluted immersion liquid was performed.

Analysis of The Porous Scaffolds

Using Mercury Porosimeter, the structural properties of the porous scaffolds were carried out. The porosity, pore size and pore size distribution of porous materials are determined using these techniques.

III. Results

Preparation of Glass Powders

Glass powders under investigation were milled and produced particle size distributions with d10, d50 and d90 values which are presented in Table (1) for the glasses prepared with and without$NH_4(HCO_3)$, respectively. It was found from the study that both glasses had a d50 of less than 40μm.

Table 1: Particle size analysis for samples sintered with and without $NH_4(HCO_3)$

Powder	particle size for glass prepared with $NH_4(HCO_3)$			particle size for glass prepared without $NH_4(HCO_3)$		
	d_{10} (μm)	d_{50} (μm)	d_{90} (μm)	d_{10} (μm)	d_{50} (μm)	d_{90} (μm)
S40B10	4.65	19.62	59.67	7.82	37.70	99.35

The XRD patterns of the prepared glass powders aftermilling is shown in the figure 1. The diffraction pattern for each glass powder is showed abroad hump band, which is a typical feature of any amorphous glassy substance and free of any major crystalline phases[3, 9, 14].

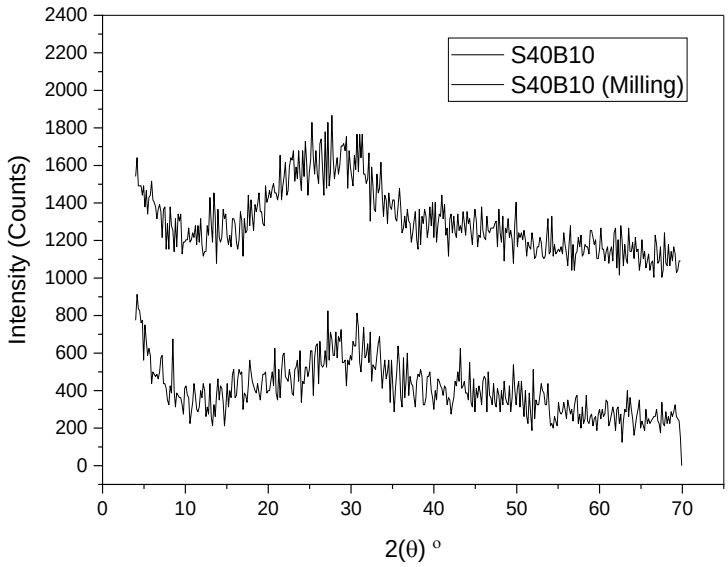

Figure 1: XRD patterns of S40B10 and S40B10 bioactive glasses prepared with and without $NH_4(HCO_3)$.

It was also noticed that, as seen by the trends of S40B10 the amorphous peak changed to lower 2 theta values after milling. The fact that calcium has a higher atomic number than phosphorus and thus disperses X-rays more easily can be attributed to this change[3, 10, 11, 12].The morphology of the prepared glass powder samples is explored using SEM analysis technique. Figure 2shows that the glassy powders were made of particles with differentshapes and dimensionswith a broad distribution of size. It is also seen that a relatively small fragments appearing sticky on the surface of larger particles[3, 5, 20].

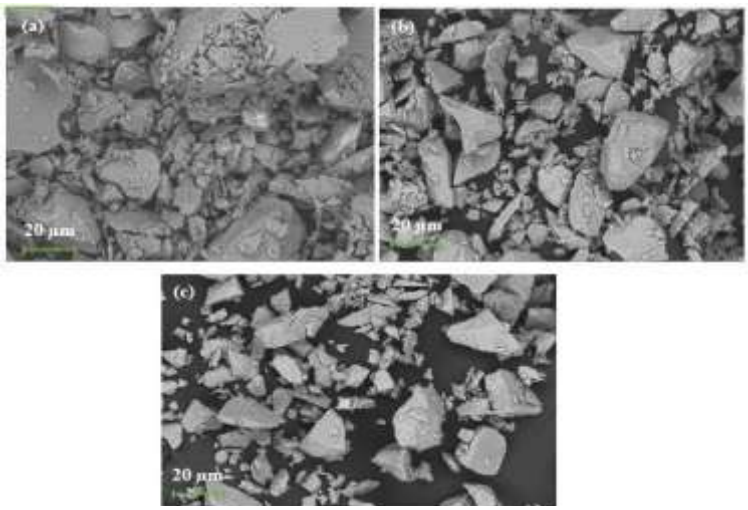

Figure 2: SEM images of S40B10 powder showing the particle size and shape prepared without NH_4 (HCO_3).

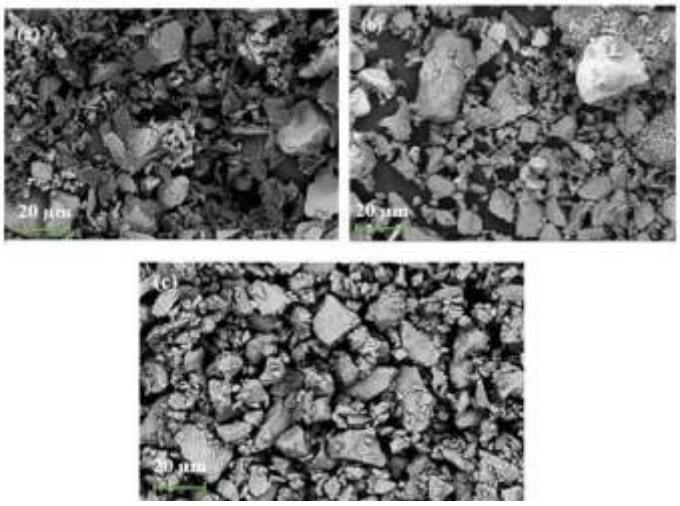

Figure 3: SEM images of S40B10 powder showing the particle size and shape prepared with $NH_4(HCO_3)$.

Figure3: represents SEM for glass sample powder which are prepared with $NH_4(HCO_3)$, we notice a similar pattern in which the amorphous and after milling hadn't noticeable crystalline phases(i.eamorphous), and the glass particles often showed differentuneven shapes with a large distribution scale

The high particle size obtained for the glasses prepared with $NH_4(HCO_3)$ was as the result of lower force used during crushing if we compareto the force used during devastating glasses which are prepared without $NH_4(HCO_3)$. Since fine particles were reported, this particle size increase was critical for improving the crystallization of bioactive glass powders[22, 23, 24, 25].

Thermal Properties of Glasses

Using a differential thermal analysis DTA, the thermal properties of the glasses, such as the glass transition temperature Tg and the initiation of crystallization Tx, were calculated. The DTA traces of the glasses (Fig. 4) is recorded on powder samples of 100-300 μm particle size at a rate of heating 10°C/min.

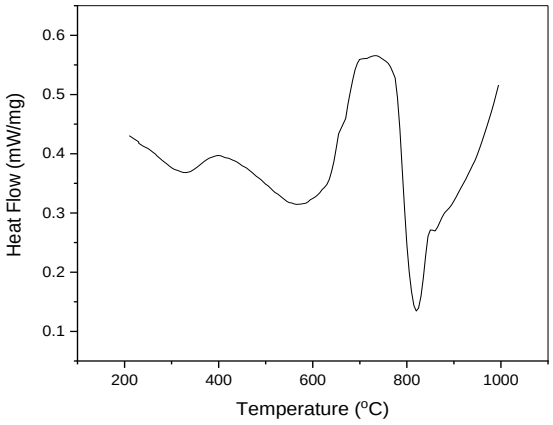

Figure 4: DTA thermographs of the glasses of investigation

DTA traces of S40B10show an endothermic effect at Tg glass transition temperature (around 580 °C); corresponding to the endotherm inflection point; followed by Tx crystallization start temperature (780°C) corresponding to the endothermic and exothermic peak inflection point[26, 27].

Sintering of Glass Powder

Samples Sintered Without Ammonium Bicarbonate $NH_4(HCO_3)$

For the aim of determining the sintering behavior of the glasses at the same time, the glass samples were sinteredwithout the foaming agent to determine the ideal sintering conditions that would be used to produce porous glass scaffolds.

Table 4 and figure 5 display the collecteddensities of sintered bioactive glasses.It was observed that the density rose to a certain temperature, accompaniedby a decrease to 600 °C after a further rise in

temperature.This means that densification atelevated sintering temperatures is hindered. The porosity behaves with oppositely to the density[3, 10, 11, 12].

Table 2: Composition, Sintering Temperature, Density, Porosity and Relative Density

Composition	**S40B10**		
Sintering temperature (°C)	500 ºC	550 ºC	600 ºC
Density (g/cm^3)	2.11±0.02	2.45±0.02	2.2±0.02
Porosity (%)	16±0.12	10±0.20	12±0.32
Relative Density (%)	82	91	84

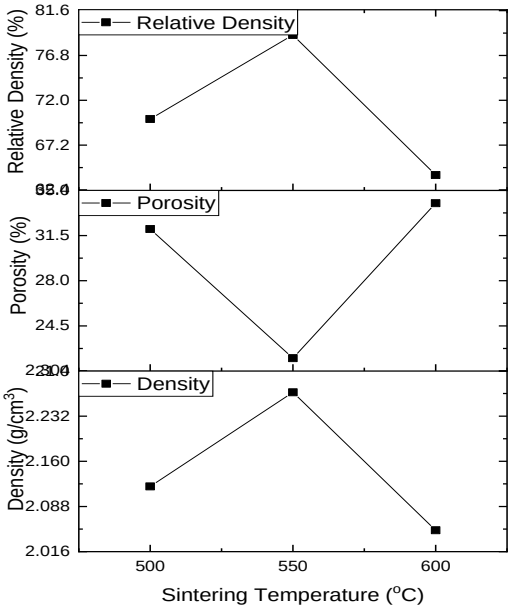

Figure 5: Density, Porosity and Relative density dependence on sintering temperature

Figure 6. XRD patterns for each sintering temperature of the bioactive glasses for S40B10. It was found from the XRD data that glass S40B10 had a similar behavior in retaining an amorphous structure at 550 °C sintering temperature.

However, by rising of sintering temperature, all the glasses, as demonstrated by appearanceof sharp diffraction peaks with marked degree ofcrystallization at 600 ° C, the samples began to crystallize.

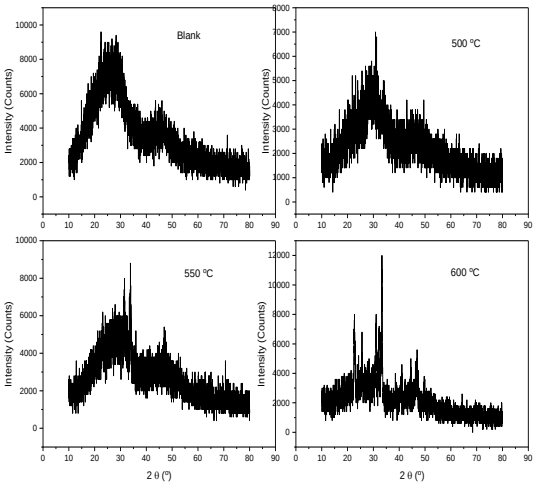

Figure 6. XRD pattern for glass S40B10 as a function of temperature

In order to analyze the microstructure of the samples following sintering, the samples werefurther characterized using SEM.

Samples sintered with $NH_4(HCO_3)$

One of the aims of this project is the manufacture of porous scaffolds that will be accomplished by sintering the glass powders with the foaming agentammonium bicarbonate $NH_4(HCO_3)$with the sole objective of raising the porosity of the scaffolds using the ideal conditions obtained from sintering the samples without ammonium bicarbonate $NH_4(HCO_3)$**.**

In the muffle furnace, the compacted pellets were sintered by applying a rate of heating of 10 °C/min at temperatures of 600 °C for S40B10 glasses at sintering temperatures with a keeping time of 1 hour. The ammonium bicarbonate $NH_4(HCO_3)$was burning before the sintering temperature for 2 hours at 68 ° C. The scaffolds obtained were characterized in density terms and the results are shown in Table 3. With increasing ammonium bicarbonate $NH_4(HCO_3)$material, the density has been observed to decrease, hence the high porosity in the samples.

TABLE 3: COMPOSITION OF SAMPLES, DENSITY, AND RELATIVE DENSITY OF SINTERED SCAFFOLDS SAMPLES

Composition	Temperature (°C)	Density (g/cm^3)	Relative Density (%)
S40B10	600	0,86±0.01	33

SEM study of cross sections was used to explain the morphology of the porous structures.The porous scaffolds of S40B10 are depicted in Figure 7.The results reveal porous microstructures with an open porosity and well-connected irregular shaped pores, resulting in a lower density.The interconnection between pores is obvious visible in the SEM- micrographs.The homogeneity of pore distribution is also visible[3, 10, 14, 23, 26].

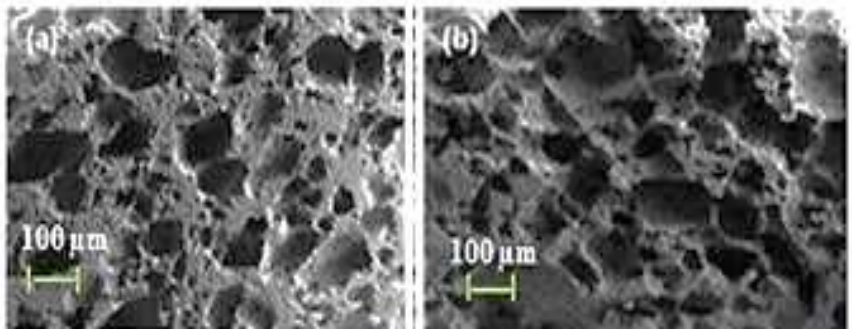

Figure 7: SEM micrographs of porous S40B10scaffolds mixed with 70 vol. % ammonium bicarbonate NH4(HCO3) sintered at 500°C for 1 hour.

IN VITRO PROPERTIES

Variation of pH

The glass tubes were submerged for 24, 48, 72 and 168 hours in simulated body fluid (SBF). Fig. 8displays the average pH of solutions SBF with S40B10 Scaffolds as a function of immersion time. Prior to immersion, the pH of SBF is 7.4. With the extended immersion time for S40B10, the pH was observed to be increased. Furthermore, the scaffold pH values with 70 vol.

The rise in pH was due to the leaching into the solution of Na^+ andCa^{2+} with the parallel formation of a SiO_2 rich layer, leading to a simpler pH[3, 10, 14, 23, 26].

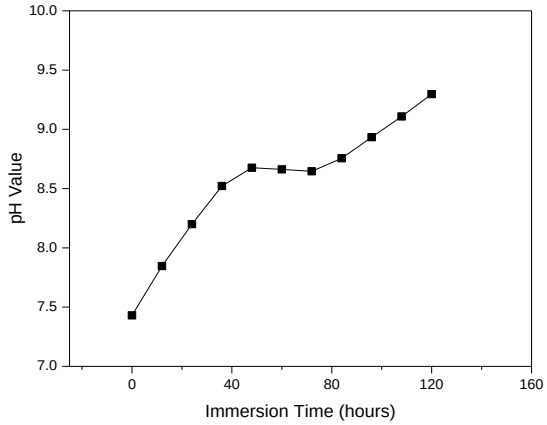

Figure 8: pH of SBF as versus immersion time for glass S40B10 scaffolds

Variation of mass

The shift in the mass of the scaffolds wasalso measured to assess how much was lost through immersion. When the scaffolds were submerged in the SBF solution, the conversion reactions and dissolution that contributed to the weight loss of the glasses were also the same reactions that regulated the pH of the solution, so it is assumed that the weight loss and pH results would indicate roughly the same pattern[4, 10, 19].

The adjustment in the weight of the S40B10as a function of the time of immersion is seen in Figure 9. It should be remembered that while S40B10 continued to show a steady rise in weight loss after theinitial dramatic increase.Whereas at lower pH levels as seen in S40B10; a lower pH was associated with a high percentage of weight loss.

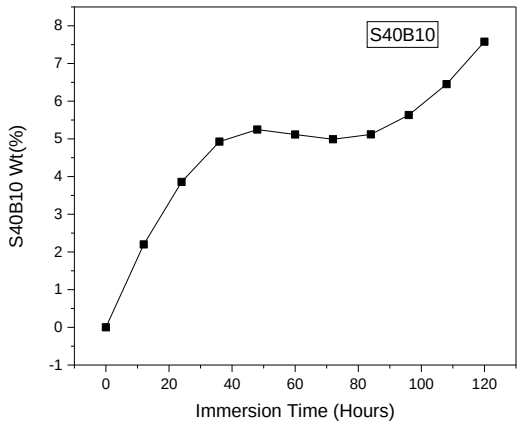

Figure 9: Weight loss (%) versus immersion time for glass S40B10 scaffolds

ICP analysis

Using inductive coupled plasma, the concentration of the ion in the immersion solution was measured during immersion.

Figure 10 shows the concentrations of (a)[Si], (b)[B], (c)P, and (d)[Ca] ions as borosilicate glass is immersed. [B], [Ca], and [Si] are all strengthened by immersion. [P], on the other hand, was found to decrease as immersion time increased.

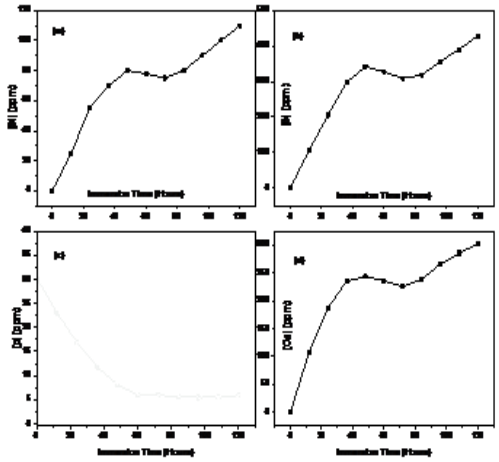

Figure 10: Ion concentration in the SBF solution of S40B10 for (a) [Si] , (b) [B], (c) [Ca] and (d) [P] versus time

Phase and Microstructural analysis

XRD analysis

To ensure that the spherical particles formed on the surfaces of the glasses were indeed HA particles; a phase analysis was carried out using XRD on the scaffolds immersed in SBF for 24, 48, 72 and 168 hours.

Figure 11: displays the XRD patterns for the S40B10 glass scaffolds. The as-prepared glass scaffolddisplayed a widely found shallow large peak, which is a typical feature of any amorphous glass content. On the other hand, the XRD patterns of the submerged samples displayed a significant peak at 36° corresponding to that of HA.

These findings indicate that SBF dissolves the scaffolds with the formation of a weak crystalline phase of $Ca_4O(PO_4)_2$. Normally, this peak is located at around 32° by using Cu K5-007; however, in this situation, the use of Co K5-007 may have induced a change in the peak location. Both peaks increased in severity as the time of immersion and porosity is increased. However, the peak intensities were still far below those for the regular crystalline HA; this strongly suggests that the as-prepared HA was partially crystallized or only weakly crystalline[3, 12, 25].

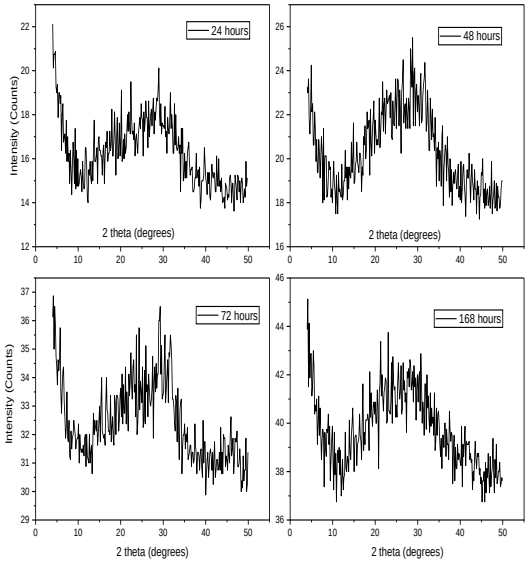

Figure 11: XRD of S40B10- $NH_4(HCO_3)$soaked in SBF for 24, 48, 72 and 168 hours

The phase analysis for glass S40B10 was conducted only on scaffolds submerged in SBF for 168 hours. The XRD were selected at 168hours to determine the formation of the HA layer only.XRD pattern of the S40B10 immersed for 168 hours remained the same as the untreated glass.This shows that SBF dissolves the scaffolding without the creation of a crystalline phase.This is obvious from the decrease in peak amplitude, the development of new peaks and the absence of certain peaks[28].

SEM images

Figure 12: displays the SEM picture and the accompanying EDX examination of one of the particles. The Ca/P ratio is calculated tobe 1.66 from the EDX study. The existence of Si and Na is most likely to come from the glass under the particles. This is predicted due to the high penetration of the X-rays.

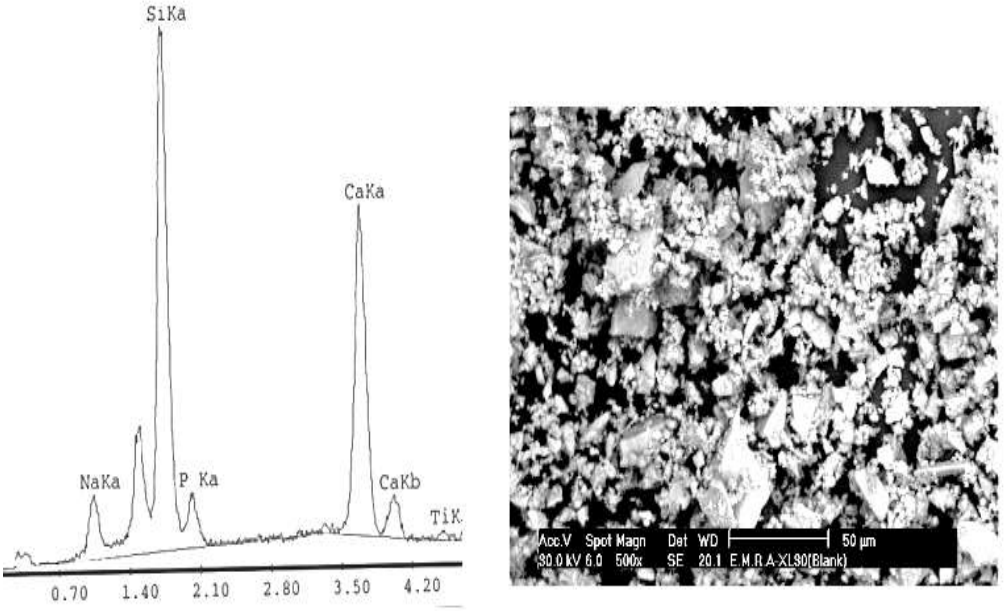

Element	Weight (%)	Atomic (%)
O	52.26	71.83
Si	9.11	5.67
Na	2.56	1.59
P	11.42	7.96
Ca	24.65	12.95

Figure 12: EDS spot analysis of HA on glass S40B10-70 vol. % $NH_4(HCO_3)$ after immersion in SBF for 24 hours

IV. Conclusions

In this article, the capacity for tissue engineering scaffolding was measuredforborosilicate (S40B10).In the past, these glasses were found to have promising antimicrobial and dissolving properties for the treatment of damaged bones. However, it is well known in tissue engineering that a large porosity and interconnected pore scaffold is needed to achieve optimum clinical application.

The crystallization and sintering capability of S40B10 was investigated without the addition of foaming agent $NH_4(HCO_3)$ at temperatures between 500°C and 600°C.Glasses S40B10 showed crystalline peaks at 540°C. Bioactive glass scaffolds with these formulations (S40B10) were developed using a foaming agent ($NH_4(HCO_3)$) with a content of 70 vol. Percent accompanied by sintering with a rate of heating 10°C/min for 1 hour at 550°C for glass samples.

It was found that, by increasing the size of the glass particles, the crystallization of glass was inhibited to some degree as observed during sintering, where no crystallization peaks were detected at 540°C for S40B10 as compared to samples sintered without ammonium bicarbonate $NH_4(HCO_3)$This suggests that the scaffolds of these two compositions have retained their amorphous character.

Despite the low weight loss of S40B10, which indicates a moderate degradation rate, S40B10 was found to have the fastest conversion rate to HA.

These glass compositionshave shown to be promising in terms of apatite formation and can be successfully processed into porous scaffolds, while maintaining their amorphous nature, which are favorable for supporting tissue ingrowth.

References:

[1]. Chatzistavrou, X., P. Newby, and A. Boccaccini, *Bioactive glass and glass-ceramic scaffolds for bone tissue engineering*, in *Bioactive glasses*. 2011, Elsevier. p. 107-128.
[2]. Fernandes, H.R., et al., *Bioactive glasses and glass-ceramics for healthcare applications in bone regeneration and tissue engineering.* Materials, 2018. **11**(12): p. 2530.
[3]. Kamal, H. and A. Hezma, *Structure and physical properties of borosilicate as potential bioactive glasses.* Silicon, 2018. **10**(3): p. 851-858.
[4]. Fiume, E., et al., *Bioactive glasses: from parent 45S5 composition to scaffold-assisted tissue-healing therapies.* Journal of functional biomaterials, 2018. **9**(1): p. 24.
[5]. Farooq, I., et al., *Bioactive glasses—structure and applications*, in *Advanced Dental Biomaterials*. 2019, Elsevier. p. 453-476.
[6]. Fernandes, J.S., et al., *Design and properties of novel substituted borosilicate bioactive glasses and their glass-ceramic derivatives.* Crystal Growth & Design, 2016. **16**(7): p. 3731-3740.
[7]. Samudrala, R., et al., *In vitro evaluation of niobia added soda lime borosilicate bioactive glasses.* Journal of Alloys and Compounds, 2018. **764**: p. 1072-1078.
[8]. Chen, Q., C. Zhu, and G.A. Thouas, *Progress and challenges in biomaterials used for bone tissue engineering: bioactive glasses and elastomeric composites.* Progress in Biomaterials, 2012. **1**(1): p. 1-22.
[9]. Coon, E., et al., *Viscosity and crystallization of bioactive glasses from 45S5 to 13‐93.* International Journal of Applied Glass Science, 2021. **12**(1): p. 65-77.
[10]. Abdelghany, A. and H. Kamal, *Spectroscopic investigation of synergetic bioactivity behavior of some ternary borate glasses containing fluoride anions.* Ceramics international, 2014. **40**(6): p. 8003-8011.
[11]. Kamal, H., *Controlling Degree Of Swelling Of Crosslinked Gelatin/Hydroxyapatite Composite For Medical Apllications.* Global Journal of Physics, 2017. **6**(2): p. 668-676.
[12]. Kamal, H., *Characterization of Silver-Borate Glasses for Biomedical Applications.* ISOR Journal of Applied Physics, 2019. **11**(3): p. 18-26.
[13]. Massera, J., et al., *Crystallization mechanism of the bioactive glasses, 45S5 and S53P4.* Journal of the American Ceramic Society, 2012. **95**(2): p. 607-613.
[14]. Rahaman, M.N., et al. *Bioactive glasses for nonbearing applications in total joint replacement*. in *Seminars in Arthroplasty*. 2006. Elsevier.
[15]. Samudrala, R., V. Penugurti, and B. Manavathi, *Cytocompatibility studies of titania-doped calcium borosilicate bioactive glasses in-vitro.* Materials Science and Engineering: C, 2017. **77**: p. 772-779.
[16]. Samudrala, R., et al., *Synthesis, characterization and cytocompatibility of ZrO2 doped borosilicate bioglasses.* Journal of Non-Crystalline Solids, 2016. **447**: p. 150-155.
[17]. Stone-Weiss, N., et al., *Combined Experimental and Computational Approach toward the Structural Design of Borosilicate-Based Bioactive Glasses.* The Journal of Physical Chemistry C, 2020. **124**(32): p. 17655-17674.
[18]. Gao, C., et al., *Preparation and in vitro bioactivity of novel mesoporous borosilicate bioactive glass nanofibers.* Journal of the American Ceramic Society, 2011. **94**(9): p. 2841-2845.
[19]. Gorustovich, A.A., J.A. Roether, and A.R. Boccaccini, *Effect of bioactive glasses on angiogenesis: a review of in vitro and in vivo evidences.* Tissue Engineering Part B: Reviews, 2010. **16**(2): p. 199-207.
[20]. Kaur, G., et al., *An introduction and history of the bioactive glasses*, in *Biocompatible Glasses*. 2016, Springer. p. 19-47.
[21]. Kokubo, T., et al., *Solutions able to reproduce in vivo surface‐structure changes in bioactive glass‐ceramic A‐W3.* Journal of biomedical materials research, 1990. **24**(6): p. 721-734.
[22]. Will, J., L.-C. Gerhardt, and A.R. Boccaccini, *Bioactive glass-based scaffolds for bone tissue engineering.* Tissue Engineering III: Cell-Surface Interactions for Tissue Culture, 2011: p. 195-226.
[23]. Xiu, T., Q. Liu, and J. Wang, *Fabrication and characterization of mesoporous borosilicate glasses with different boron contents.* Journal of materials research, 2007. **22**(7): p. 1834-1838.
[24]. Yao, A., et al., *Preparation of bioactive glasses with controllable degradation behavior and their bioactive characterization.* Chinese Science Bulletin, 2007. **52**(2): p. 272-276.
[25]. Yao, A., et al., *In vitro bioactive characteristics of borate‐based glasses with controllable degradation behavior.* Journal of the American Ceramic Society, 2007. **90**(1): p. 303-306.
[26]. Anderson, P.W., B. Halperin, and C.M. Varma, *Anomalous low-temperature thermal properties of glasses and spin glasses.* Philosophical Magazine, 1972. **25**(1): p. 1-9.
[27]. Baino, F., S. Hamzehlou, and S. Kargozar, *Bioactive glasses: where are we and where are we going?* Journal of functional biomaterials, 2018. **9**(1): p. 25.
[28]. Kamal, H., *Electro paramagnetic resonance and magnetization measurements of metal-substituted hydroxyapatites used in hyperthermia applications.* Journal of Advances in Physics. **13**(7).

H.Kamal, et. al. "Characterization of Porous Borosilicate Bioactive Glasses for Medical Applications." *IOSR Journal of Pharmacy and Biological Sciences (IOSR-JPBS)*, 16(2), (2021): pp. 13-19.